

# A multi-layer zone model for predicting temperature distribution in a fire room<sup>\*</sup>

CHEN Xiaojun<sup>\*\*</sup>, YANG Lizhong, DENG Zhihua and FAN Weicheng

(State Key Laboratory of Fire Science, University of Science and Technology of China, Hefei 230026, China)

Received September 7, 2003; revised February 12, 2004

**Abstract** A multi-layer zone fire growth model is developed to predict the vertical distributions of the temperature in a single room. The fire room volume is divided into a number of horizontal layers, in which the temperature and other physical properties are assumed to be uniform. The principal equations for each laminated horizontal layer are derived from the conservation equations of mass and energy. The implemented fire sub-models are introduced, including the combustion, fluid flow and heat transfer models. Combined with these sub-models, the zone equations for the gas temperature of each layer are solved by Runge-Kutta method for each time step. The results of the sample calculations compare well with the results of experiments conducted by Steckler et al.

**Keywords:** compartment fire, multi-layer zone model, fire prediction, temperature field.

Modeling of fire in a compartment can be achieved either using a zone modeling method or a computational fluid dynamics (CFD) modeling method. The most common zone model is the two-zone model. The main character of this model is that it divides the room(s) into a hot, upper layer and a cooler, lower layer, and that the physical properties of each layer, such as its gas temperature and species concentrations are all uniform. Some models of this type have been developed<sup>[1~3]</sup>, and a comprehensive review of the existing two-zone fire models can be found in reference [4]. The computational fluid dynamics (CFD) model can predict temperature and velocity field profiles throughout the domain of interest<sup>[5]</sup>. Three-dimensional time-dependent equations describing the fluid dynamics can be solved numerically under the surface conditions specific to the problem. An advantage of CFD models is that they can predict details of temperature and velocity distributions in the domain of interest, while zone models can only give average temperatures in only one layer or two. Moreover, CFD models need tremendous CPU time. In a complicated case, it might take more than a couple of days to simulate only one minute of the real fire process.

In a room fire experiment, a stratified layer situation can be observed, but the layer interface is not always clear and the temperature varies rather gradually with height. Therefore, if a model is available for

predicting the vertical temperature profile, more accurate analyses of fire may be possible with a reduced computation time.

In this study, a new zone modeling approach, which we call the multi-layer zone model, is proposed to predict vertical distributions of temperature in a fire compartment. In this model, the space volume in a compartment is divided into an arbitrary number of layers as the control volumes (see Fig. 1), and the physical properties, such as temperature and species concentrations in each layer are assumed to be uniform. The boundary walls are also divided into segments in accordance with the layer division. The radiation heat transfer between the layers, and between the layers and the wall segments are calculated, as well as the convective heat transfer between the layers and the wall segments. This model still retains the advantages of zone models and it is expected to be useful for practical applications on fire safety design of buildings.

## 1 Governing equations

The concept of the multi-layer zone model is illustrated in Fig. 1. One notable difference of the model from the existing two-layer zone models is that the fire plume flow does not mix with the upper layer as soon as it penetrates a layer interface, but continues to rise until it hits the ceiling, and then it pushes

<sup>\*</sup> Supported by the NKBRSF project of China (Grant No. 2001CB409603)

<sup>\*\*</sup> To whom correspondence should be addressed. E-mail: xjchen@ustc.edu.cn

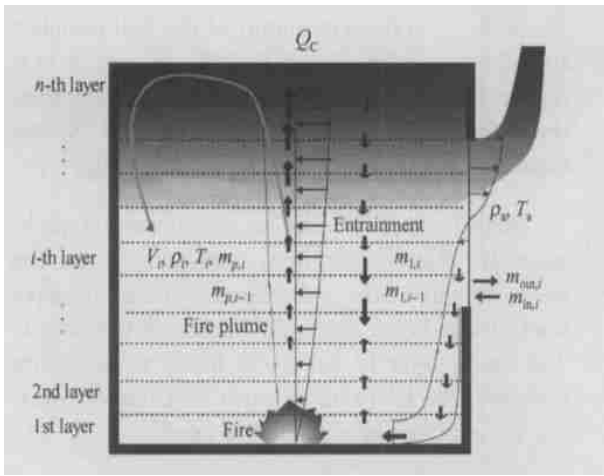


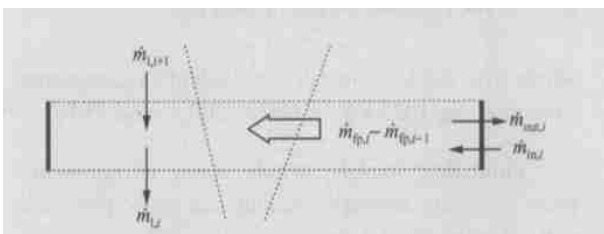
Fig. 1. Illustration of the multi-layer zone model.

down the gases in the top layer. Like the two-zone models, the principal equations for each laminated horizontal layer are derived from the conservation equations of mass, internal energy, and species fraction.

From Fig. 2, we obtain the mass conservation equation:

$$\frac{d}{dt}(\rho_i V_i) = -(\dot{m}_{fp,i} - \dot{m}_{fp,i-1}) + \dot{m}_{1,i+1} - \dot{m}_{1,i} - \dot{m}_{out,i} + \dot{m}'_{in,i}, \quad (1)$$

where  $\rho_i$  and  $V_i$  are the density and volume of the  $i$ -th ( $1 \leq i \leq n-1$ ) layer;  $\dot{m}_{fp,i}$  is the mass flow rate at the  $i$ -th and the  $(i+1)$ -th layer interface inside the fire plume. The term  $\dot{m}_{fp,i} - \dot{m}_{fp,i-1}$  denotes the rate of mass entrained into the fire plume from the  $i$ -th layer;  $\dot{m}_{1,i}$  is the net mass flow rate from the  $i$ -th layer to the  $(i-1)$ -th layer through the surface outside the fire plume;  $\dot{m}_{out,i}$  is the mass flow rate flowing out through the opening from the  $i$ -th layer, and  $\dot{m}'_{in,i}$  is the mass gain rate of the  $i$ -th layer transported by the cold plume from the opening. For the top layer, considering that the mass rate of gas entrained into the fire plume is eventually transported to this layer, the mass conservation becomes

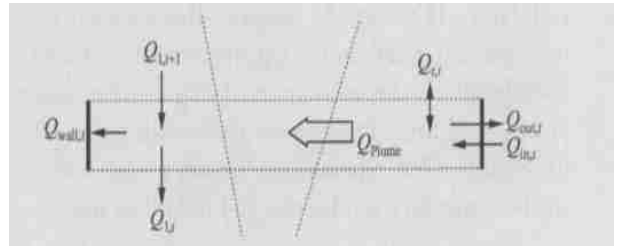
Fig. 2. Mass conservation of  $i$ -th layer.

$$\frac{d}{dt}(\rho_n V_n) = \sum_{i=1}^{n-1} (\dot{m}_{fp,i} - \dot{m}_{fp,i-1}) - \dot{m}_{1,n} - \dot{m}_{out,n} + \dot{m}'_{in,n}. \quad (2)$$

From Fig. 3, we obtain the energy conservation equation

$$\begin{aligned} \frac{d}{dt}(C_p \rho_i V_i T_i) = & -C_p(\dot{m}_{fp,i} - \dot{m}_{fp,i-1})T_i \\ & + C_p\{\max(\dot{m}_{1,i+1}T_{i+1}, 0) \\ & + \min(\dot{m}_{1,i+1}T_i, 0)\} \\ & - C_p\{\max(\dot{m}_{1,i}T_i, 0) \\ & + \min(\dot{m}_{1,i}T_{i-1}, 0)\} - C_p\dot{m}_{out,i}T_i \\ & + C_p\dot{m}'_{in,i}T_{air} - Q_{w,i} + Q_{r,i}, \end{aligned} \quad (3)$$

where  $C_p$  is the specific heat;  $T_i$  is the temperature of the  $i$ -th layer,  $Q_{w,i}$  is the convection heat loss to the wall surface from the  $i$ -th layer,  $Q_{r,i}$  is the net radiation heat gain of the  $i$ -th layer. The second and third terms show that, if  $\dot{m}_{1,i+1}$  is positive, the net flow through the interface of the  $(i+1)$ -th and the  $i$ -th layers is downward, otherwise upward.

Fig. 3. Energy conservation of  $i$ -th layer.

For the top layer, considering that the heat released by the combustion is transported to the layer through the fire plume, the energy conservation is written as:

$$\begin{aligned} \frac{d}{dt}(C_p \rho_n V_n T_n) = & C_p \sum_{i=1}^{n-1} \{(\dot{m}_{fp,i} - \dot{m}_{fp,i-1})T_i\} \\ & - C_p\dot{m}_{1,n}T_n - C_p\dot{m}_{out,n}T_n \\ & + C_p\dot{m}'_{in,n}T_{air} - Q_{w,n} + Q_{r,n} + Q_c. \end{aligned} \quad (4)$$

Considering that a fire is basically a phenomenon at atmospheric pressure, the equation of state of the ideal gas in this model is simplified as:

$$\rho_i T_i = \text{const}. \quad (5)$$

Note that the left-hand side of Eq. (3) can be expanded as:

$$\frac{d}{dt}(C_p \rho_i V_i T_i) = C_p \rho_i V_i \frac{dT_i}{dt} + C_p T_i \frac{d(\rho_i V_i)}{dt}.$$

The zone governing equation for temperature of each layer is derived by substituting Eqs. (1) and (3) into Eq. (6), and we obtain

$$\begin{aligned} \frac{dT_i}{dt} = & \frac{1}{\rho_i V_i} \{ \dot{m}_{1,i} T_i - \dot{m}_{1,i+1} T_i \\ & + [\max(\dot{m}_{1,i+1} T_{i+1}, 0) + \min(\dot{m}_{1,i+1} T_i, 0)] \\ & - [\max(\dot{m}_{1,i} T_i, 0) + \min(\dot{m}_{1,i} T_{i-1}, 0)] \\ & + \dot{m}'_{in,i} (T_{air} - T_i) \} + \frac{Q_{e,i} - Q_{w,i}}{C_p \rho_i V_i}. \end{aligned} \quad (7)$$

For the top layer, substituting Eqs. (2) and (4) into Eq. (6) yields

$$\begin{aligned} \frac{dT_n}{dt} = & \frac{1}{\rho_n V_n} \left\{ \sum_{i=1}^{n-1} [\dot{m}_{p,i} - \dot{m}_{p,i-1}] T_i \right. \\ & \left. - \sum_{i=1}^{n-1} [\dot{m}_{p,i} - \dot{m}_{p,i-1}] T_n + \dot{m}'_{in,n} (T_{air} - T_n) \right\} \\ & + \frac{Q_c + Q_{e,n} - Q_{w,n}}{C_p \rho_n V_n}. \end{aligned} \quad (8)$$

## 2 Fire models

Equations (5), (7) and (8) can be integrated using Runge-Kutta method for the temperature of each layer. However, to complete this equation system, the rate terms in the equations must be formulated based on the relevant modeling of component processes of fire. This section deals with these sub-fire models. The implemented fire sub-models include the heat transfer, combustion and fluid flow models.

Heat transfer models include conduction heat transfer, convection heat transfer and radiation heat transfer models.

To calculate the conduction heat transfer through the compartment boundaries, a one-dimensional and transient conduction model is used. The governing equation is as follows:

$$\begin{aligned} \frac{\partial T_{w,i}}{\partial x} &= \frac{k_w}{c_w \rho_w} \cdot \frac{\partial^2 T_{w,i}}{\partial x^2}, \\ -k_w \frac{\partial T_{w,i}}{\partial x} \Big|_{x=0} &= \dot{q}_{w,i} + \dot{q}_{rw,i}, \\ -k_w \frac{\partial T_{w,i}}{\partial x} \Big|_{x=l} &= \dot{q}_{wout,i} + \dot{q}_{rwout,i}, \end{aligned}$$

where  $k_w$ ,  $\rho_w$  and  $c_w$  are the thermal conductivity, density and specific heat of boundaries.

In the compartment, the rate of the convection heat transfer from the  $i$ -th layer to the wall boundary is calculated by

$$q_{w,i} = h(T_i - T_{w,i,0}) A_{w,i},$$

where  $T_{w,i,0}$  is the temperature of the wall boundary around the  $i$ -th layer, and  $h$  is the convection heat transfer coefficient and  $h$  is computed using empirical correlations based on Grashof, Prandtl and Nusselt numbers. The details can be found in Ref. [2].

Radiation heat transfer is a very important mechanism in compartment fires, especially in the fire room. In this work, a three-surface model of upper layer, lower layer, and wall fraction is introduced. The smoke layer is considered to be an absorptive medium. The following radiation heat transfer equation for each surface element  $k$  is used<sup>[6,7]</sup>

$$\begin{aligned} \sum_{j=1}^N \left[ \frac{\tilde{q}_j}{\epsilon_j} - F_{k-j} \frac{1 - \epsilon_j}{\epsilon_j} \tilde{\alpha}_{k-j} \right] q_j \\ = \sum_{j=1}^N [(\tilde{q}_j - F_{k-j} \tilde{\alpha}_{k-j}) \sigma T_j^4 - F_{k-j} \tilde{\alpha}_{k-j} \sigma T_g^4], \end{aligned}$$

$$Q_g = - \sum_{k=1}^N A_k q_k,$$

where  $q_j$  is the net radiation heat transfer rate of surface  $j$ ;  $\epsilon_j$  is the emissivity of surface  $j$ ;  $\tilde{q}_j$  is the Kronecker delta,  $\tilde{q}_j = 1$ , when  $k = j$ , and  $\tilde{q}_j = 0$ , when  $k \neq j$ ;  $F_{k-j}$  is the view factor from surface  $k$  to  $j$ ;  $T_j$  and  $T_g$  are the temperatures of surface  $j$  and gas;  $\tilde{\alpha}_{k-j}$  and  $\tilde{\alpha}_{k-j}$  are geometrical mean transmittance and absorptance from surfaces  $k$  to  $j$ ;  $q_1$ ,  $q_2$  and  $q_3$  can be calculated by solving linear algebraic equations using Gauss-Jordan elimination method.

The combustion models deal with the heat release rate of combustible materials in a compartment. The heat release rate in unconstrained combustion can be obtained by

$$Q_c = \dot{m}_b \cdot \Delta H \cdot \chi,$$

where  $\Delta H$  is the effective heat of combustion per unit kilogram fuel in open air,  $\dot{m}_b$  is the mass burning rate, and  $\chi$  is efficiency factor which takes into account incomplete combustion.

For a wide range of fires, the fire growth can be accurately represented by a set of specific T-squared fires<sup>[8]</sup> labeled slow, medium, and fast

$$Q_c = \alpha t^2,$$

where  $\alpha$  is the fire intensity coefficient, representing fires reaching 1055 kW in 600 s, 300 s, and 150 s.

Fluid flow models include plume entrainment, mass flow rate through opening and mass flow rate through surfaces of layers.

Fire-induced buoyant plume entrainment is a

very important factor in modelling fire growth and smoke spread in a building. A number of formulas can be found in Refs. [ 9 ~ 11] . Zukoski' s model is used as default in this model

$$m_p = 0.21 \left( \frac{\rho_{\infty}^2 g}{c_p T_{\infty}} \right)^{1/3} \dot{Q}_c^{1/3} z^{5/3},$$

where  $\dot{Q}_c$  (kW) is the heat release rate, and  $z$  is height from floor.

Mass flow through a vertical vent is driven by the pressure difference between the two sides of the vent, and it can be calculated by integrating Bernoulli' s equation along the vertical direction of the vent<sup>[12]</sup>,

$$\dot{m}_{out} = \frac{2}{3} A \sqrt{H} C_d \rho_0 \sqrt{2g \frac{T_0}{T} \left( 1 - \frac{T_0}{T} \right)} \left( 1 - \frac{N}{H} \right)^{3/2},$$

where  $A$  and  $h$  are the area and height of this part of vent,  $C_d$  is the coefficient of vent flow, which is typically taken as 0.7 and  $N$  is the neutral plane location.

The enthalpy flow rate through the surface of the top layer to the lower layer outside the fire plume is obtained using Eq. (8) and Eq. (5)

$$\begin{aligned} h_n = & \sum_{i=1}^{n-1} \{ (\dot{m}_{p,i} - \dot{m}_{p,i-1}) T_i \} - \dot{m}_{out,n} T_n \\ & + \dot{m}_{in,n}' T_{air} + \frac{1}{C_p} (\dot{Q}_c + \dot{Q}_{r,n} - \dot{Q}_{w,n}). \end{aligned}$$

The enthalpy flow rate through the interface of the  $(i+1)$ -th and the  $i$ -th layer is calculated layer by layer, using the enthalpy flow rate through the upper surface as follows:

$$\begin{aligned} h_i = & - (\dot{m}_{p,i} - \dot{m}_{p,i-1}) T_i + h_{i+1} - \dot{m}_{out,i} T_i \\ & + \dot{m}_{in,i}' T_{air} + \frac{1}{C_p} (\dot{Q}_{r,i} - \dot{Q}_{w,i}). \end{aligned}$$

When  $h_i$  is negative, the net flow through the surface is upward, otherwise downward. Thus the net mass flow rate through the surface is

$$\begin{cases} \dot{m}_{l,i} = \frac{h_i}{T_i} & (h_i \geq 0), \\ \dot{m}_{l,i} = \frac{h_i}{T_{i-1}} & (h_i < 0). \end{cases}$$

### 3 Model prediction and comparison with experiments

#### 3.1 Examples of model predictions

An example of model prediction is presented here. The input data of the model are shown in Table 1. The

compartment is divided into 8 layers. The fire is assumed to be slow T-squared fires<sup>[8]</sup> at 1055 kW. It reaches its maximum at 600 s and remains stable at 1800 s, then it decays to zero at 3600 s. The predicted temperature history of each layer is shown in Fig. 4.

Table 1. Model input data for a single compartment example

	Dimensions		
	Depth(m)	Width(m)	Height(m)
Compartment	3.0	4.0	3.0
Opening	N/A	0.8	2.0
	Physical and thermal properties of compartment boundaries		
	Ceiling	Wall	Floor
Thickness(cm)	20	15	15
Density (kg/m <sup>3</sup> )	1600	1600	1600
Conductivity (W/mK)	0.8	0.7	0.7
Specific heat (J/kg·K)	840	840	840
Surface Emissivity	0.8	0.8	0.8

The ambient conditions of pressure and temperature are 101, 300 Pa and 20 °C, respectively.

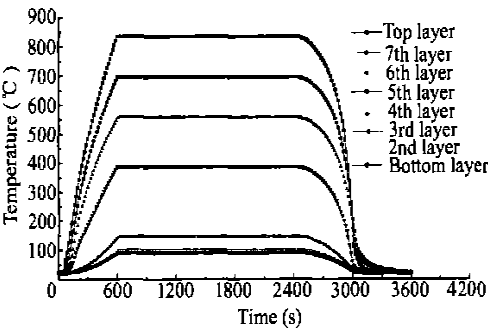


Fig. 4. Predicted temperature history. (Room: 3 m×4 m×3 m, Door: 0.8 m×1.8 m; Fire: Medium T-Square Fire (1 MW); Layer number: 8).

#### 3.2 Comparison with experimental data

Steckler et al.<sup>[13]</sup> carried out a series of fire experiments within a compartment to investigate fire induced flows. The experimental data obtained from these fire tests have been used as part of the validation process for both zone model and CFD model. The data represents non-spreading fires in small compartments. A series of 45 experiments were conducted by Steckler et al. to investigate fire induced flows in a compartment 2.8 m×2.8 m in plane and 2.18 m in height (see Fig. 5). The walls and ceiling were 0.1 m thick and they were covered with a ceramic fibre insulation board to establish nearly steady state conditions within 30 minutes. The series of experiments consisted of a gas burner placed systematically in 8 different floor locations with a variety of single compartment openings ranging from small windows to wide doors. The door openings are 0.24 m to

0.99 m. The 0.3 m diameter burner was supplied with commercial grade methane at fixed rates producing constant fire strengths of 31.6, 62.9, 105.3 and 158 kW.

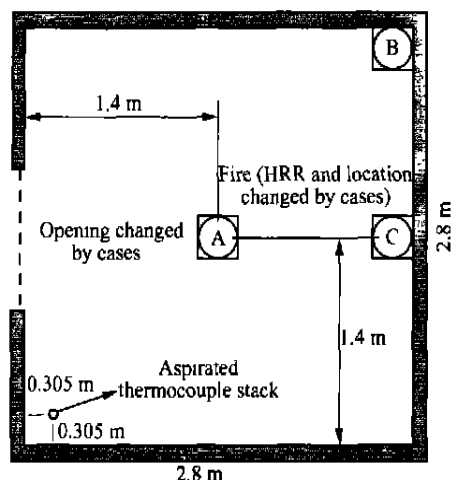


Fig. 5. Setup of Steckler's experiment.

The conditions of the calculations such as the geometry of the walls and the opening, the initial air temperature in the compartment and the heat release rate are determined basically by the experimental conditions for each case. The room volume is divided into 18 layers. The flow rate through surfaces of layers, the temperature of gas is calculated at every 0.1 second. Fig. 6 shows the vertical distribution of the temperature from the experiment (Test 14, HRR 62.9 kW, 6/6 Door and Fire at location A) at steady state stage and predictions by the model at 1000 sec. (when it is almost in steady-state). The predicted temperature distributions of the room at 1000 sec. generally agree with the experiment (also for other cases). However, the hot upper layers are thinner by 0.1 ~ 0.3 m than the experiments. This is influenced mainly by the accuracy of fire models especially plume entrainment and mass flow rate through opening models. A continuing effort should be made to refine the model.

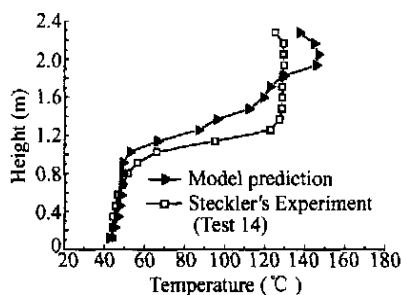


Fig. 6. Predicted vertical distribution of the temperature compared with experiment. (Room: 2.8 m × 2.8 m × 2.18 m, Door: 0.74 m × 1.83 m; HRR: 62.9 kW; Layer number: 18).

## 4 Conclusions

The multi-layer zone model is based on the concept of zone models but different with the two-zone models. Comparisons of this model with experiment show that the model is applicable for engineering purpose. As we expected, it is more detailed and accurate than two-zone models and it is less time-consuming than Field models.

## References

1. Fu, Z. M. et al. A two-zone fire growth and smoke movement model for multi-compartment buildings. *Fire Safety Journal*, 2000, 34(3): 257.
2. Peacock, R. et al. CFAST—The consolidated model of the fire growth and smoke transport. NIST Technical Note, 1993, 1299.
3. Walton, W. D. Zone computer fire models for enclosures. In: SFPE Handbook of Fire Protection Engineering (ed. DiNenno, P. J.), Quincy, MA: National Fire Protection Association, 1995.
4. Friedman, R. An international survey of computer models for fire and smoke. *J. Fire Prot. Eng.*, 1992, 4: 81.
5. Novozhilov, V. Computational fluid dynamics modeling of compartment fires. *Progress in Energy and Combustion Science*, 2001, 27(6): 611.
6. Siegel, R. Thermal Radiation Heat Transfer. 2nd ed. Washington, DC: Hemisphere Publishing Corporation, 1981.
7. Hoover, J. B. et al. An improved radiation transport submodel for CFAST. *Combustion Science and Technology*, 1997, 127(1~6): 213.
8. Schiffliti, R. P. et al. Design of detection systems. In: SFPE Handbook of Fire Protection Engineering (ed. DiNenno, P. J.), Quincy, MA: National Fire Protection Association, 1995.
9. McCaferey, B. J. Momentum implications for buoyant diffusion flames. *Combust Flame*, 1983, 52: 149.
10. Zukoski, E. E. Mass flux in fire plumes. In: Proceedings of the Fourth International Symposium on Fire Safety Science, International Association for Fire Safety Science, 1994.
11. Heskestad, G. Fire plumes. In: SFPE Handbook of Fire Protection Engineering (ed. DiNenno, P. J.), Quincy, MA: National Fire Protection Association, 1995.
12. Rockett, J. A. Fire induced gas flow in an enclosure. *Combustion Science and Technology*, 1976, 12: 165.
13. Steckler, K. D. et al. Flow induced by fire in a compartment. NBSIR 82-2520, Nat. Bur. Stand. 1982.